Corner Detection Based on Gradient Correlation Matrices of Planar Curves

Xiaohong Zhang*, Hongxing Wang, Andrew W. B. Smith, Brian C. Lovell

Abstract --- An efficient and novel technique is developed for detecting and localizing corners of planar curves. This paper begins with a discussion of the gradient feature distribution of planar curves, followed by constructing Gradient Correlation Matrices (GCMs) over the region of support (ROS) of planar curves. It is shown that the eigen-structure and determinant of GCMs encode the geometric feature of the curves, such as curvature features and dominant points. Further, the determinant of the GCM is defined as the "cornerness" measure of planar curves. A comprehensive performance evaluation of the proposed detector is performed using the ACU and Error Index criteria. The corresponding results demonstrate that the GCM detector has a strong corner position response, and possesses better detection and localization performance than several traditional methods.

Index Terms **--- Corner Detection, Gradient Correlation Matrix, Planar Curves, Determinant, Region of Support.**

I. INTRODUCTION

Corners are important features in images and are frequently used for: scene analysis, stereo matching, robot navigation, stitching of panoramic photographs, and object tracking. There are many competing algorithms for detecting corners in images. Since the pioneering work of Förstner [1], and Harris and Stephens [2], the structure tensor of image gradients, denoted by P, has become popular for corner detection. For example, Rohr [4-5] developed a rotationally invariant corner detector based solely on the determinant of P. Tomasi [6-7] proposed a corner detector based on the smallest eigenvalue of P. Recently, Kenney [8] defined a reciprocal value of the smallest eigenvalue of P as a "cornerness" measure according to condition number theory. Moreover, Kenney [3] discussed and reviewed five detectors, and presented an axiomatic approach to corner detection based on the structure tensor of image gradients. The structure tensors in all of these detectors have been used rather successfully to find corners in images, and applications in invariant region detection or shape detection [24-26] have also been reported. However, these structure tensors are calculated from image intensities and are computationally expensive. A computationally efficient method for calculating structure tensors with equivalent characteristics is an important research area.

Corner detection approaches can be split into two groups, intensity based methods and boundary based

*Manuscript received 15.07.2008. The work described in this paper was partially supported by the National Natural Science Foundation of China (Grant No. 60604007) Corresponding Author: Xiaohong Zhang (e-mail: xhongz@yahoo.com.cn), is with School of Software Engineering, Chongqing University, Chongqing, 400030, P. R. China. Hongxing Wang is with College of Mathematics & Physics, Chongqing University. Andrew Smith is with the School of Information Technology and Electrical Engineering, The University of Queensland, Australia. Brian Lovell is with the School of Information Technology and Electrical Engineering and NICTA.

methods [9-22]. Intensity based methods act directly on the image, while boundary methods act on extracted edges. Tsai [9] proposed a boundary based corner detector using the eigenvalues of covariance matrices of contour coordinate points over the Region of Support (ROS). It requires that the radius of the ROS is large enough to suit the statistical characteristic of Tsai's detector. However, too large a radius may miss small features and cause aliasing to occur; while too small a radius may cause the detector to suffer from sensitivity to noise. In addition, exact computation of the eigenvalues of covariance matrices is computationally expensive. Classical techniques for corner detection of planar curves include: Curvature Scale Space (CSS) [10-15], wavelet transformations of contour orientation [16-19], and eigenvectors of covariance matrices [20]. With the exception of the eigenvector method, these methods based on curvature estimation require calculating higher order derivatives of the smoothed versions of plane curves, and suffer from sensitivity to noise. Moreover, an appropriate scale is difficult to choose to appropriately suppress noise. These problems can be overcome using the structure tensor of planar curve gradients. While the structure tensor of *image gradients* is widely used for a variety of low-level image features, to the best of our knowledge no reports on the structure tensor of *planar curve gradients* for corner detection have been presented in the literature

In this paper we develop a new algorithm for corner detection based on the structure tensor of planar curve gradients. Similar to the well-known Förstner and Harris detectors, the proposed detector computes the structure tensor of the gradient and seeks corners at the maxima of its determinant. Instead of using the image gradient however, the proposed detector uses the contour's tangent vector. The Gradient Correlation Matrix (GCM) formulated using Lagrange multipliers only requires calculation of the first derivative of the planar curves. Avoiding the higher order derivatives reduces the effect of noise. A small ROS may then be used to improve corner localization and to prevent nearby features from merging. Consequently, the proposed detector overcomes the aforementioned problems associated with the existing CSS, wavelet, and covariance matrix detectors, and offers better detection and localization performance. The main contributions and

organization of this paper are as follows:

- Firstly, we introduce the motivation for using GCMs by analyzing the gradient feature distribution in the plane spanned by the gradients of plane curves, and formulate the GCM by least squares and the Lagrange multiplier method, where the GCM is viewed as the structure tensor of planar curve gradients.

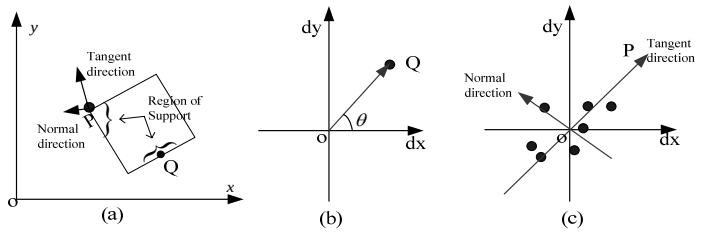

Fig.1: Illustration of the basic idea of GCM, (a) a planar curve and a region of support centered at point P; (b) the plane spanned by gradients of planar curves and the gradient vector corresponding to the center point P; (c) the gradient vector distribution over the ROS and the corresponding major gradient vector and normal vector.

- Secondly, we analyze the geometric properties of GCM based on the typical corner models [10] and find that local maxima of the determinant of GCM correspond to the positions of the dominant points. Therefore, we define the determinant of GCM as a cornerness measure of planar curves.
- Finally, we perform a comprehensive evaluation of the detection and localization performances of the detectors. The GCM corner detector outperforms the CSS, and wavelet, and covariance matrix detectors according to the ACU [11] and the Error Index [23] criteria.

II. GRADIENT CORRELATION MATRIX (GCM)

A. Motivation

Considering a regular planar curve $C(t) = (x(t), y(t))$ (1)

parameterized by t, where $x(t), y(t)$ are coordinate functions. Then, from (1) the gradient vector at any point on the curve can be expressed as:

$$C'(t) = (x'(t), y'(t)) = (dx, dy) \qquad (2)$$

where dx, dy are the gradients of the planar curve $C(t)$ in the x and y directions. In the following section we will discuss an intuitive observation for the relationship between the dominant points of planar curves and the

gradient distribution for a set of gradient vectors over the ROS.

If we think of any gradient vector in a ROS as a point in a plane described by axes *dx* and *dy*, the distribution of gradient vectors for all points in the ROS will reflect the local feature structure. As an illustration, Fig. 1(a) shows a planar curve and ROS centered at two points *P* and *Q* on the curve, and tangent and normal directions with respect to P. Fig. 1(b) shows the plane spanned by *dx* and *dy*, and that the gradient vectors over the ROS for the point *Q* converge to an identical orientation. Fig. 1(c) indicates the distribution of the gradient vectors over the ROS for the point *P*, and the corresponding major gradient and normal orientations, which are required to pass through the origin and fitted using the gradient vectors. From Figs. 1(b) and 1(c), it follows that the distribution of the gradient vectors converges to a direction if the ROS in the neighborhood of any center point is straight line segment; while the distribution scatters around the origin if the ROS contains a corner.

Based on the above intuitive observation, we regard the gradient vector with respect to planar curve coordinates as a distribution in the two-dimension plane, and construct the corresponding gradient correlation matrices (GCM) of planar curves. These matrices describe the local geometric features of planar curves, such as normal and tangent directions, and dominant points. Then, according to the eigen-structure and properties of the GCM, we present a simple and effective cornerness measure for planar curves.

Remark 1. In fact, when we regard any image gradient vector as a point in the plane spanned by image gradients, we obtain a similar geometric explanation. Hence, the structure tensor of image gradients can be derived by our approach.

B. Gradient Correlation Matrix Calculation

We now consider the set of gradient vectors over the ROS of a planar curve $(dx_i, dy_i)^T$, $i = 1, \cdots, k$. Characterizing the line of best fit by its unit normal vector $\boldsymbol{n}$, the perpendicular distance between each point (dx_i, dy_i) and the line of best fit is equal to the projection of the point onto $\boldsymbol{n}$, where the distance is: $d_i^2(\boldsymbol{n}) = (\boldsymbol{n}^T \begin{bmatrix} dx_i & dy_i \end{bmatrix}^T)^2$. To find the line of best fit, we minimize the sum of the squared perpendicular

distances: $\varepsilon^2 = \sum_{i=1}^{k} d_i^2(\boldsymbol{n}) = \boldsymbol{n}^T M \boldsymbol{n}$ (3)

where $M = \sum_{i=1}^{k} (dx_i, dy_i)^T (dx_i, dy_i)$. (4)

Performing constrained minimization using a Lagrange multiplier and minimizing (3), subject to $\boldsymbol{n}^T \boldsymbol{n} = 1$. We then have $2M\boldsymbol{n} - 2\lambda\boldsymbol{n} = 0$, i.e., $M\boldsymbol{n} = \lambda\boldsymbol{n}$. (5)

In this paper *M* is referred to as Gradient Correlation Matrix (GCM). From (5), it can be seen that the line of best fit is equivalent to the principal eigenvector of M. Moreover, it is not difficult to show that the minimal eigenvalue of *M* reflects the distribution feature or the degree of dispersion of the gradient vectors in the gradient plane. Therefore, M characterises the local geometric features of any planar curve.

Remark 2. The GCM is typically regarded as the standard outer product of the planar curve gradients, an extension of the structure tensor of image gradients. As such the GCM is built using the set of *contour gradients* in the ROS, $X_{GCM} = \left\{ (dx_{-k}, dy_{-k})^T, \ldots, (dx_k, dy_k)^T \right\}$, where *k* is the radius of ROS. This is different from covariance matrix based approaches [9, 20], which are built from the set of *contour points* in the ROS, $X_{COV} = \left\{ (x_{-k}, y_{-k})^T, \ldots, (x_k, y_k)^T \right\}$. While these forms become analogous when the expectation is subtracted from X_{COV}, they remain quite distinct.

III. Properties of GCM and the Corner Detection Algorithm

To determine the relationship between the GCM and the dominant points of planar curve, further investigation into the properties of M is required. Here, we used the two typical corner models presented by Rattarangsi [10], which are treated as isolated segments to simplify the investigation. Figs. 2(a) and 2(b) show the Γ-corner model and the END model respectively. Note that if the width of the ROS is small enough any complex corner models of planar curves can be treated as a combination of the two models. Assuming that $C(t)$ is a continuous differential curve, we can redefine the

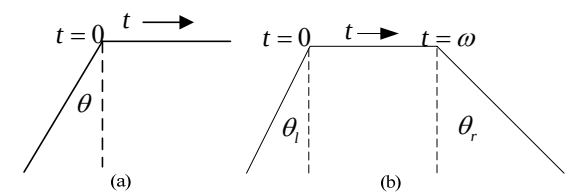

Fig. 2(a) Γ-corner model (b) END corner model

GCM in (4) as the auto-correlation matrix between dx and dy, that is:

$$M(t)=\left\langle \begin{bmatrix} dx \\ dy \end{bmatrix} \begin{bmatrix} dx & dy \end{bmatrix} \right\rangle = \begin{bmatrix} \langle d^2x \rangle & \langle dxdy \rangle \\ \langle dxdy \rangle & \langle d^2y \rangle \end{bmatrix}. \quad (6)$$

where $\langle * \rangle \equiv \int_{t-W}^{t+W} * ds$ indicates an integral operation on the small interval [t-W, t+W] at the center point t, and $2W$ is the width of integral interval. It is then trivial to show that the eigenvalues of M (hence the determinant) are invariant to translation and rotation.

In the following, the relationship between the determinant of $M(t)$ and dominant points of a planar curve will be discussed based on Γ and END models.

A. Γ*-Corner Model*

Consider the Γ-corner model, in which two straight line segments intersect at a corner:

$$x(t)=\begin{cases} t\sin\theta & t<0 \\ t & t\geq 0 \end{cases} \quad \text{and} \quad y(t)=\begin{cases} t\cos\theta & t<0 \\ 0 & t\geq 0 \end{cases} \quad (7)$$

where t is the arc length parameter, and θ is the angle between one straight line and the vertical axis as shown in Fig. 2(a). A straight line segment is then a special case of the Γ corner model where θ is equal to 90^o.

Property 1. The determinant of $M(t)$, $\det(M(t))$, will reach a unique maximum at the intersection where t equals 0, i.e., there exists a unique maximum at the corner.

In fact, from (6) and (7) we can express $M(t)$ as:

if $t-W<0$ and $t+W>0$,

$$M(t)=\begin{bmatrix} (W-t)\sin^2\theta+t+W & (W-t)\sin\theta\cos\theta \\ (W-t)\sin\theta\cos\theta & (W-t)\cos^2\theta \end{bmatrix}$$

else, $M(t)=0$

Thus, the determinant of $M(t)$ can be rewritten as

$$\det(M(t))=\begin{cases}(W^2-t^2)\cos^2\theta & (t-W<0)\text{ and }(t+W>0)\\ 0 & \text{otherwise}\end{cases}$$

Clearly, $\det(M(t))\le W^2\cos^2\theta\ \ \forall t$. It is easy to verify that the unique maximum of $\det(M(t))$ is equal to $W^2\cos^2\theta$ if and only if $t=0$, i.e., Property 1 holds.

As a special case of Γ-corner model, we reach the following conclusion for a line segment model.

Property 2. For a line segment, $\det(M(t))=0$.

B. END Model

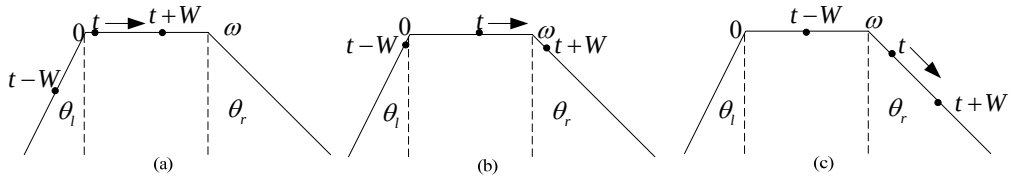

Fig. 3 Relationship diagrams between the integral interval and the corners of END model. (a), (b) and (c) show which intervals contain θ_l and θ_r respectively.

Let us consider another model, which contains two corners θ_l and θ_r are separated by a width of ω, as shown in Fig. 3. This model is represented by:

$$x(t)=\begin{cases}t\sin\theta_l & t<0\\ t & 0\le t<\omega\\ (t-\omega)\sin\theta_r+\omega & w\le t\end{cases}\qquad y(t)=\begin{cases}t\cos\theta_l & t<0\\ 0 & 0\le t<\omega\\ (\omega-t)\cos\theta_r & w\le t\end{cases}\qquad (8)$$

If $2W\le\omega$, we may regard the *END* model as two conjoint and independent Γ models because any integral interval of (6) contains at most one corner. If $2W>\omega$, as shown in Fig. 3(b), some integral interval of (6) must contain both corners. Based on this, we only consider the situation when $2W>\omega$ for the END model. First, when $W+\omega\le t$ or $t<-W$, we obtain:

$$\det(M(t))=0. \qquad (9)$$

Second, for $-W\le t<\omega-W$ as shown in Fig. 3(a), the interval only contains the corner θ_l and we get:

$$M(t)=(W-t)\begin{bmatrix}\sin^2\theta_l & \sin\theta_l\cos\theta_l\\ \sin\theta_l\cos\theta_l & \cos^2\theta_l\end{bmatrix}+\begin{bmatrix}(t+W) & 0\\ 0 & 0\end{bmatrix}$$

and

$$\det(M(t)) = (W^2 - t^2)\cos^2\theta_l . \qquad (10)$$

Third, for $\omega - W \le t < W$ as shown in Fig. 3(b), the interval contains both corners θ_l and θ_r. We then have:

$$M(t) = (W-t)\begin{bmatrix} \sin^2\theta_l & \sin\theta_l\cos\theta_l \\ \sin\theta_l\cos\theta_l & \cos^2\theta_l \end{bmatrix} + (t+W-\omega)\begin{bmatrix} \sin^2\theta_r & \sin\theta_r\cos\theta_r \\ \sin\theta_r\cos\theta_r & \cos^2\theta_r \end{bmatrix} + \begin{bmatrix} \omega & 0 \\ 0 & 0 \end{bmatrix}$$

and:

$$\det(M(t)) = \left(-t^2 + \omega t - W(W-\omega)\right) \times (\sin\theta_l\cos\theta_r + \sin\theta_r\cos\theta_l) \quad (11)$$

Finally, for $W \le t < W + \omega$ as shown in Fig. 3(c), the interval only contains the corner θ_r and we get:

$$M(t) = (t+W-\omega)\begin{bmatrix} \sin^2\theta_r & -\sin\theta_r\cos\theta_r \\ -\sin\theta_r\cos\theta_r & \cos^2\theta_r \end{bmatrix} + \begin{bmatrix} (W-t+\omega) & 0 \\ 0 & 0 \end{bmatrix}$$

and:

$$\det(M(t)) = (W^2 - (t-\omega)^2)\cos^2\theta_r . \qquad (12)$$

From (8)-(12), it follows that $\det(M(t))$ has three local maxima at $t = 0, \omega/2$, and ω. However, the point at $t = \omega/2$ is a false corner.

Property 3. For the END model, if the width of the integral interval *W* satisfies $2W \le \omega$, the determinant of $M(t)$ has three local maxima at $t = 0, \omega/2$, and ω.

Remark 3. In general, for discrete planar curves the width of integral interval is chosen to be 3, i.e., $2W + 1 = 3$. Thus, as the distance between any two corners must be more than 2 the false corner at $\omega/2$ will not occur. Property 3 can be derived from other corner models, such as the STAIR model [8], in a similar fashion. From properties 1-3, it follows that $\det(M(t))$ may be defined as a cornerness response function for the corners of planar curves. We then have the following corner detection algorithm.

C. GCM Corner Detection Algorithm

1) Utilize a good edge detector to extract edge contours $C(t)$ from the original image.

2) Extract the edge contours from the edge image and:

   a) Fill gaps in the edge contours.

b) Locate the T-junctions and mark them as T-corners.

3) Smooth the curves using Gaussian a kernel with standard derivation σ to remove noise and trivial details.

4) Calculate the cornerness response function as described in section 3,

5) Determine the corners by comparing the local maxima of $\det(M(t))$ with a threshold value.

All parameter values used in the experimental evaluation were determined from either existing work, or based on our empirical study (see Section IV-C for details).

IV. Performance Evaluation And Experiments

In this section we present the results of two experimental evaluations. First, we summarize the experimental results of the parameter setting for the proposed GCM detector. Second, we compare the performance of the proposed GCM corner detector with five existing corner detectors: (i) CSS [11], (ii) Wavelet transforms [17], (iii) eigenvalues of covariance matrices [9], (iv) eigenvectors of covariance matrices [20], and (v) the well-known Harris detector [2]. For convenience, we denote these detectors as: CSS, Wavelet, Eigenvalue, Eigenvector, and Harris.

In our experiments, all the detectors were set with their default best parameter values. For fair comparisons, all boundary based detectors were applied using the same edge extraction and selection step. Experiments were performed on both original images and their "degraded" (geometric transformed and noise disturbed) images. Ground truth corner sets were created by visual inspection. The number of true detections, the number of corners that were missed (false non-detections), and the number of false detections were collected. For geometric transformations, we transformed the ground truth corners using the transformation parameters prior to matching. Finally, corners detected in a 3×3 neighborhood of the true corners were considered as matches. The performance of the detectors was evaluated using two metrics: Accuracy (ACU) [13] and the Error Index [23].

A. Evaluation criteria

Mohanna and Mokhtarian [13] proposed the ACU accuracy criterion which takes into account of the number of corners in the original image as well as the number of corners in each of the transformed images.

Letting N_o denote the number of the corners detected in the original image ($N_o \neq 0$), N_g the number of the true corners, and N_a the number of the correctly matched corners. The ACU accuracy criterion is:

$$\text{ACU} = \left(N_a / N_o + N_a / N_g \right) / 2 \times 100\%$$

As advocated by Sojka [23], not only did we evaluate the number of corners correctly detected (true detections), but also the number of corners that were missed (false non-detections) and the number of false detections. False detections occur when a corner is detected at a point near which no true corner exists. The total error of the detector is defined to be the sum of the false non-detections and false detections, and the Error Index is the ratio of total error to the number of true corners in the image.

B. Image database

We examine a total of 20 different original gray-level images including: Block, House, Lab, Pentagon, Airplane, Flower, Leaf, Gear, Key, Fish, Shark, and simple planar curves. Many of these original images were collected from standard databases [9-21]. In addition to these original images, we used 1720 test images obtained by applying five types of "degradations" on each original image:

Rotation - The original image was rotated with rotation angles chosen by sampling the interval [-80°, +80°] at a 10° resolution.

Uniform scaling - The original image was scaled with scale factors chosen by sampling the interval [0.5,1.5] at a resolution of 0.1.

Non-uniform scaling - The x-scale and y-scale parameters were independently chosen by sampling the interval [0.5, 1.5].

Planar affine transforms - Planar affine transforms were applied using: rotation angles in the interval [-10°, +10°], non-uniform scaling with *x* and *y* scale parameters chosen in the interval [0.5, 1.5] at a resolution of 0.1.

Gaussian noise - Zero mean Gaussian white noise was added to the original image. Variances were chosen by sampling the interval [0.005, 0.05] at a resolution of 0.005.

Therefore, we used 20 original, 320 rotated, 200 uniform scaled, 400 non-uniform scaled, 600 rotated and scaled transformed images, and 200 Gaussian noised images.

C. Parameter Settings

In this section, we summarize the experimental results of the parameter settings for the proposed GCM detector. To extract good boundaries, we used the edge detection and contour tracking methods suggested by Mokhtarian [11] as the first two steps of the algorithm.

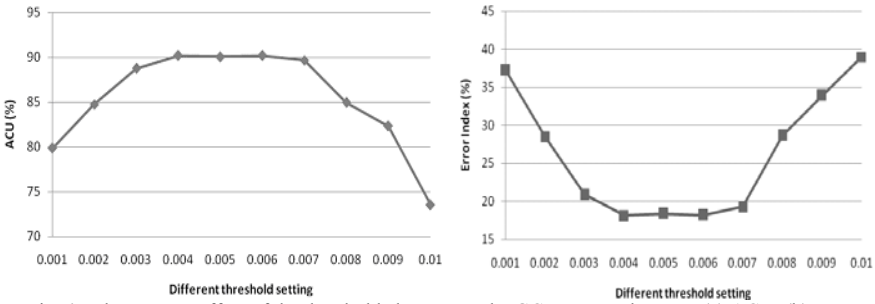

Fig. 4: The average effect of the threshold changes on the GCM corner detector; (a) ACU, (b) Error Index

The purpose of the third step is to reduce the effect of noise, such as quantization and random noise. The width of the Gaussian function indicates the scale of the smoothed contours, and should be small enough to retain real corners and to leave their positions unchanged. Interestingly, we discovered that a small width could be used, with good detection and localization performance. This is due to strong cornerness response function given in equation (6). For instance, the standard derivation σ was chosen to lie between 2 and 3.5, with 3 commonly used in our experiments. In the fourth step, the ROS radius was set to 1 for calculating the cornerness response of curves; hence the ROS width was equal to 3. The gradient operator in (5) was implemented using central differencing, with the central difference for the sequence $\{x_i\}$ given by: $\Delta x_i = 0.5(x_{i+1} - x_{i-1})$. A threshold value of 0.005 was chosen for the final step. We will discuss how this threshold was decided using the following experiments, all of which were performed on the original images.

TABLE I. PARAMETERS OF THE COMPARATIVE DETECTORS

	GCM	CSS	Eigenvalue	Eigenvector	Wavelet	Harris
Threshold:	0.005	0.05	1	0.2	0.2	1300
ROS radius:	1	-	10	10	-	10

Fig. 4 shows the average

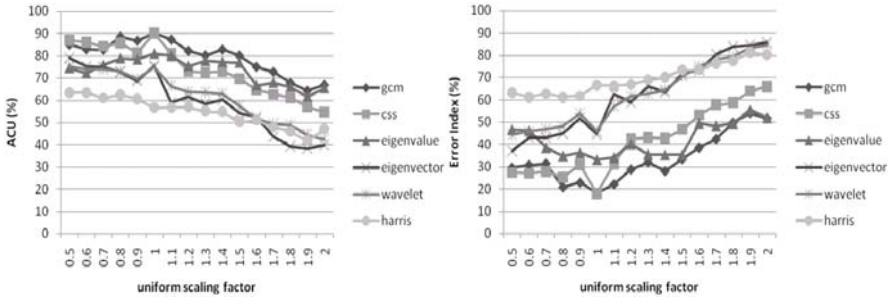

Fig. 7. ACU and Error Index values for uniform scaling. (a) ACU, (b)Error Index.

effect of the threshold changes on the GCM corner detector. The smaller the threshold, the fewer corners detected. At low thresholds, the GCM detector detects too many weak/noisy false corners, resulting in a low ACU and a high Error Index. At high thresholds, the GCM detector missed too many true corners, again resulting in a low ACU and a high Error Index. From Fig. 4, the ACU value increases to a stable maximum in the interval [0.004, 0.006], and the Error Index value is also minimized in this interval. Therefore, we empirically choose .005 as the default threshold for the GCM detector as it offers the highest robustness (maximum ACU and minimum Error Index). Other selected parameters for the various detectors are summarized in table I.

D. Experimental Results

Fig. 5 shows the average and overall ACU and Error Index under different geometric transformations and Gaussian noise. The proposed GCM's ACU is above 75% under each attack, and the Error Index is approximately 35%. This is an improvement in both ACU and the Error Index error metrics on the detectors used for comparison. The results for: rotation, uniform scaling, and Gaussian noise are presented in greater detail in Figs. 6-8. Fig. 6 shows that each of the detectors is approximately invariant to rotations, except for the Eigenvector detector. Fig. 7 shows that the effectiveness of each detector decreased gradually as the scaling factors diverged from unity. Figure 8 shows the effectiveness of each detector decreasing considerably with increasing Gaussian noise variance.

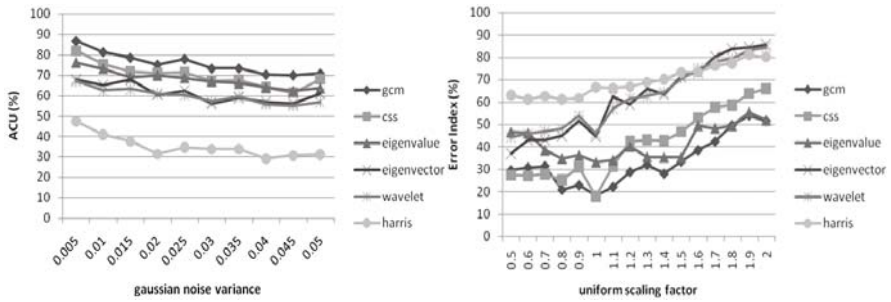

Fig.8. ACU and Error Index values for noise disturbing. (a) ACU, (b)Error Index.

E. Discussion

We have discussed several problems associated with existing detectors based on the structure tensor of image intensity: CSS, Wavelet, and covariance matrix based detectors, and described a novel and robust

GCM corner detector based on the structure tensor of planar curve gradients. The computation of the detectors using the structure tensors of image intensities is expensive; CSS and wavelet detectors require up to the second order derivative for calculating the cornerness measure, while the covariance matrix based detectors require a large ROS to reduce the impact of noise. In our experiments we found that over 80 percent of the GCM detector's computational time was spent performing edge detection, while calculating the cornerness measure was quite efficient as it requires only first order derivatives. A Gaussian function with a small scale may reduce this effect to some degree. In addition, the GCM is formulated using least squares and Lagrange multipliers, and is shown to be robust to the various attacks. A small ROS radius (1 in the experiments) can be used by the proposed detector to improve corner localization and to avoid missing conjoint corners. It is vital that the structure tensor reflects the local structure features of planar curves, which is ensured because of the GCM's intuitive geometric characteristics. As a result, GCM obtained higher localization performance and lower error rates than the competing detectors.

V. Conclusion

In this paper we have presented a novel corner detection algorithm, using gradient correlation matrices (GCMs) of planar curves, which has been shown to perform significantly better than competing methods on our dataset. The approach is based on an intuitive observation of the distribution of gradient vectors of planar curves. Gradient correlation matrices of planar curves have been derived using least squares and Lagrange multipliers, and are defined as the standard structure tensor of planar curve gradients. These extend the existing structure tensors of image gradients. Moreover, it has been shown that the determinant of the GCMs is an effective cornerness response function using the Γ and END corner models. The determinant of the GCMs then forms the basis of our simple and efficient corner detection algorithm. The GCM method has several advantages over those more commonly used. For instance, both the Gaussian smoothing parameter and the ROS radius can be kept small, improving the detection and localization performance. Additionally, only the first order derivative of the planar curve is required, reducing both the impact of noise and computational cost. Finally, experiments have illustrated that the proposed detector has better detection and

localization performances under different scales, rotations, and noise disturbances, than several well-known methods.

REFERENCES

[1] W. Förstner, “A feature based correspondence algorithm for image matching”, International Archives of Photogrammetry and Remote Sensing, vol.26, pp.150-166, 1986.

[2] C. Harris and M. Stephens, “A combined corner and edge detector”, Proc. of the 4th ALVEY vision conference, pp.147, University of Manchester, England, 1988

[3] C. S. Kenney, M. Zuliani, and B. S. Manjunath, “An axiomatic approach to corner detection”, Proc. CVPR'05. vol.1, pp.191, 2005.

[4] K. Rohr, “On 3d differential operators for detecting point landmarks’, Image and Vision Computing, vol. 15, no.3, pp.219-233, 1997.

[5] K. Rohr, “Localization properties of direct corner detectors”, J. of Mathematical Imaging and Vision, vol. 4, no.2, pp.139-150, 1994.

[6] C. Tomasi and T. Kanade, “Shape and motion from image streams under orthography—a factorization method”, International Journal on Computer Vision, vol. 9, no.2, pp.137-154, 1992.

[7] J. Shi and C. Tomasi, “Good features to track”, In Proc. Of IEEE Conf. on Computer Vision and Pattern Recognition (CVPR’94), pp.593, Seattle, Washington, June 1994.

[8] C. Kenney, B. Manjunath etc., “A condition number for point matching with application to registration and post-registration error estimation”, IEEE Transactions on Pattern Analysis and Machine Intelligence, vol.25 no.11, pp.1437-1454, 2003.

[9] Tsai, D. M., Hou, H. T., H. J. Su, “Boundary-based corner detection using eigenvalues of covariance matrices,” Pattern Recognition Letters, vol. 20, pp.31-40, 1999.

[10] Rattarangsi and R. T. Chin, “Scale-based detection of corners of planar Curves”, IEEE Trans. on Pattern Analysis and Machine Intelligence, vol. 14, pp .430-449, 1992.

[11] Mokhtarian, F., Suomela, R., “Robust image corner detection through curvature scale space”, IEEE Trans. on Pattern analysis and Machine Intelligence, vol. 20 pp. 1376-1381, 1998.

[12] Mokhtarian F. and Suomela R., “Enhancing the curvature scale space corner detector, Proc. Scandinavian Conf. on Image Analysis, ” pp.145-152, 2001.

[13] Mohanna, F., and F. Mokhtarian, “Performance evaluation of corner detection algorithms under similarity and affine transforms,” Proc. British Machine Vision Conference, pp. 353-362, 2001.

[14] He, X. C., Yung N. H. C., “Curvature scale space corner detector with adaptive threshold and dynamic region of support, ” IEEE Proceedings of the 17th International Conference on Pattern Recognition, pp. 791-794. 2004.

[15] Zhang, X. H., Lei, M., Yang, D., etc., “Multi-scale Curvature Product for Robust image Corner Detection in Curvature Scale Space,” Pattern Recognition Letters, vol. 28, pp. 545-554. 2007.

[16] Chen, C. H., Lee, J. S., Sun, Y., “Wavelet transformation for gray-level corner detection, Pattern Recognition,” vol. 28 pp. 853−861, 1995.

[17] Lee J. S., Sun Y. N., Chen C. H., “Multiscale Corner detection by using wavelet transform,” IEEE Trans. Image Processing, vol. 4, pp. 100-104, 1995.

[18] Quddus A., Gabbouj M., “Wavelet-based corner detection technique using optimal scale,” Pattern Recognition Letters, vol. 23 pp. 215-220, 2002.

[19] Gao X. T., Sattar F., Quddus A., and Venkateswarlu R., “Multiscale contour corner detection based on local natural scale and wavelet transform,” Image and Vision Computing, vol.25, no.6, pp 890-898, 2007.

[20] Chi-Hao Yeh “Wavelet-based corner detection using eigenvectors of covariance matrices,” Pattern Recognition Letters, vol. 24, pp. 2797-2806, 2003

[21] Asif. Masood and M. Sarfraz, “Corner detection by sliding rectangles along planar curves,” Computers & Graphics, vol.31, no.3, pp. 440-448, 2007.

[22] F. Arrebola and Francisco Sandoval, “Corner detection and curve segmentation by multi-resolution chain-code linking,” Pattern Recognition, vol. 38, no.10, pp.1596-1614, 2005

[23] E. Sojka, “A new and efficient algorithm for detecting the corners in digital images”, Lecture Notes in Computer Science，Springer Berlin, vol. 2449, pp.125-132, 2002.

[24] K. Mikolajczyk, K. and C. Schmid, "Scale and affine invariant interest point detectors", International Journal of Computer Vision, vol.60, no.1, pp: pp 63-86, 2004.

[25] K. Mikolajczyk, T. Tuytelaars, C. Schmid etc., “A comparison of affine region detectors”, International Journal of Computer Vision, vol.65, no.1/2,pp:43-72, 2005

[26] T. Lindeberg, "Feature detection with automatic scale selection", International Journal of Computer Vision, vol.30, no.2, pp: 77-116, 1998.